JOURNAL OF Applied Polymer SCIENCE

Synthesis and Characterization of a Conducting Polyaniline/TiO_2-SiO_2 Composites

Fuwei Liu,[1] Zhi Liu,[1] Yanhong Gu,[1] Zhe Chen,[2] Pengfei Fang[1]

[1]Department of Physics and Key Laboratory of Artificial Micro- and Nano-structures of Ministry of Education, Wuhan University, Wuhan 430072, China

[2]Department of Material Science and Engineering, Wuhan Institute of Technology, Wuhan 430073, China

Correspondence to: Pengfei Fang (E-mail: fangpf@whu.edu.cn)

ABSTRACT: Polyaniline/TiO_2-SiO_2 composites were prepared by an *in situ* chemical oxidation polymerization approach in the presence of hybrid TiO_2-SiO_2 fillers. The obtained polyaniline/TiO_2-SiO_2 composites were characterized by scanning electron microscopy (SEM), transmission electron microscopy (TEM), Fourier transform infrared spectrometer (FTIR), X-ray diffraction (XRD), thermogravimetry (TG), and current−voltage (I−V) measurements. SEM picture shows a variation in morphology of polyaniline (PANI) from fiber shape to relatively regular particle shape with increasing TiO_2-SiO_2 contents in the composites. The floccule-like structures were observed by high resolution TEM, which may help improve the efficiency of conductive network. SEM, XRD, TG, and FTIR spectra all reveal that a relatively strong interaction exist between TiO_2-SiO_2 and PANI. The I−V characteristics in such composites indicate that the charge transport is mainly governed by the space charge effects, which occurs at the interface between the conducting PANI and TiO_2-SiO_2. Meanwhile, PANI/TiO_2-SiO_2 composites exhibit significant increase in conductivity than PANI/TiO_2 or PANI/SiO_2. The reasons about high conductivity of PANI/TiO_2-SiO_2 have also been discussed. © 2013 Wiley Periodicals, Inc. J. Appl. Polym. Sci. 130: 2288–2295, 2013

KEYWORDS: conducting polymers; surfaces and interfaces; composites

Received 9 December 2012; accepted 17 April 2013; Published online 20 May 2013
DOI: 10.1002/app.39425

INTRODUCTION

Polyaniline (PANI) has been intensively studied as one of the most promising conducting polymer matrixes because of its inherent properties such as ease of synthesis, relatively cheap prices, good environment stability. And, most recently, polyaniline−inorganic conducting composites have been widely used in various electrical and electronic devices. Meanwhile, various attempts have been made to prepare polyaniline−inorganic composites to improve the conductivity of PANI. Su et al.[1] synthesized PANI/TiO_2 composites with high conductivities, and found that the conductivity increased after thermal treatment at 80°C. Zengin et al.[2] prepared PANI/SiO_2 conductive films whose conductivity are much higher than that of the neat PANI. The conductivities reach the maximum value when the content of SiO_2 is 10 wt %. Lira-Gantu et al.[3] have reported that the addition of V_2O_5 improved the conductivity of PANI from 10^{-6} to 10^{-2} S/cm in PANI/V_2O_5 composites. The relationship between conductivity property and critical parameters (e.g., reaction temperature, reaction time) was also investigated. All these results are very encouraging. It has also been noted that some conductive PANI composites exhibit novel properties such as positive temperature coefficient of resistance, photocurrent, piezoresistivity, and photosensitivity.[4–12] In most cases, the main objective is to obtain a sufficient level of conductivity in the material. Besides the polymerization conditions of PANI, the interaction between organic and inorganic phases, or the characteristics of inorganic fillers are also main factors affecting the conductivity properties of these composites. For example, the morphologies and particle sizes of metal oxide fillers are found to affect the electrical properties of PANI composites. Some fine-grade powders such as crystalline titanium dioxides are believed to help induce the formation of a more efficient network for charge transport, but the interaction between the organic and inorganic phase is relatively weak.[13,14] While small fillers (e.g., amorphous silica) can avoid flaws of weak cohesion. However, these small fillers are severely aggregated and some time can diminish the extent of conjugation of PANI macromolecules, thus their conductivities are restricted.[15,16] Until now, the microstructure design of high performance PANI remains a challenge.

In this article, TiO_2-SiO_2 hybrid fillers were prepared and used as starting building units to obtain PANI composites by an in

situ polymerization method. The fine-grade commercial TiO_2 P25 (about 25 nm in diameter) is able to combine with relatively small porous fumed silica through reflux treatment in deionized water. Fumed silica with fluffy structures is easy to form chemical Si−O−Ti bond and/or increase the adsorption onto the surface of fine-grade P25 particles, and thus can modify and connect P25 particles to form network-like structures. On the other hand, large surface area of fumed silica can adsorb aniline molecules and enhance the interaction between the organic and inorganic phases. These help to get more efficient cross-linked network for charge transport and enhance the electrical and electronic properties of PANI composites. The characterization and electrical properties of PANI/TiO_2−SiO_2 composites were also investigated.

EXPERIMENTAL

Preparation of PANI/TiO_2−SiO_2 Composites

TiO_2 (P25, Degussa; 1.2 g, 15 mmol) is placed in a round-bottom flask with equimolar amount of fumed silica (CAB-O-SIL M-5, Cabot Corporation). Deionized water (250 mL) was added, and the powders were bath sonicated for 30 min, followed by reflux with stirring for 5 h. After cooling the sample was centrifuged, collected, and dried in a vacuum oven at about 40°C for 24 h.

A certain quantity of TiO_2−SiO_2 powder was dispersed in 90 mL of 1 mol/L HCl by sonication for 1 h, and followed by stirring for 0.5 h. Then 1 mL purified aniline (ANI) was added to the HCl solution, and the obtained solution was transferred to an ice bath environment. An appropriate amount of ammonium persulfate (APS, 2.5 g) was dissolved in 100 mL of 1 mol/L HCl, and the solution was transferred to an ice bath environment. The pre-cooled aqueous solution of APS was added dropwise to the pre-cooled aniline–acid mixed solution with constant stirring. The reaction was conducted at 5 ± 1°C. After the addition, the stirring was continued for 1 h for ensuring complete polymerization. Then the reaction products were purified using deionized water and methanol. The reaction products were washed with deionized water and centrifuged to separate PANI. Separated PANI was then dispersed in deionized water and centrifuged. This treatment was repeated several times until the suspension reached a neutral pH and became colorless. The resulting polyaniline precipitate was centrifuged and repeatedly washed using methanol to remove the oligomer and finally dried in oven at about 60°C for 24 h.

About 0.15, 0.30, 0.45, and 0.60 g TiO_2−SiO_2 powder were added to synthesize PANI/TiO_2−SiO_2 composites with different TiO_2−SiO_2/ANI molar ratios (1 : 5, 2 : 5, 3 : 5, and 4 : 5) which were abbreviated as PANI-15, PANI-30, PANI-45, and PANI-60, respectively. PANI without TiO_2−SiO_2 was also synthesized under the same condition.

We also synthesized PANI/TiO_2 and PANI/SiO_2 (initial molar ratios TiO_2/ANI = 1 : 2; SiO_2/ANI = 1 : 2) using the same method to compare with characteristics of PANI/TiO_2−SiO_2.

Characterizations

The morphologies of the PANI and PANI/TiO_2−SiO_2 composites were investigated by a Sirion field-emission scanning electron microscopy (FE-SEM). More detailed morphology of PANI-60 was also investigated with transmission electron microscopy (TEM) on a JEM2010 instrument (JEOL, Japan). The samples for TEM were prepared by the ultrasonic dispersion of the powder in ethanol and then the coating of the dispersing solution onto wholly carbon-coated copper grids.

The molecular structures of PANI, PANI/TiO_2, PANI/SiO_2, and PANI/TiO_2−SiO_2 composites were studied by an attenuated total reflectance Fourier transform infrared spectrometer (ATR-FTIR, Nicolet iS10). The scan range is from 550−4000 cm^{-1}, number scans were 32, and the resolution used was 6 with data spacing of 1.929 cm^{-1}. The X-ray diffraction (XRD) curves of these samples were recorded by a Bruker D8 Advanced XRD instrument (Bruker AXS, Germany) under the conditions of 40 kV and 30 mA, by the Cu $K\alpha$ monochromatic radiation with a wavelength of 1.5406 Å, after scanning in the 2θ range of 8−80° (scanning rate is 4°/min) at intervals of 0.02. The thermal stability of all PANI/TiO_2−SiO_2 samples were characterized by a Netzsch STA449C Simultaneous Thermal Analyzer (NETZSCH, Germany) from 25 to 800°C with a heating rate of 10°C/min under air atmosphere with flow rate of 20 mL/min.

A small quantity (0.4 g) of the obtained PANI and PANI/TiO_2−SiO_2 powders was compacted at 8 MPa pressure in order to make thin disc specimens for Current−Voltage (I−V) measurements. The specimens were mounted in the electrometer/high resistance meter (Keithley 6517A) which was coupled to a computer. Different steel blocks of known weight were placed on the top of the specimen (silver and aluminum foil electrodes were used for contacts) to obtain the effect of pressure on the resistance. The details of the measurement has been described elsewhere.[4,5,12,17,18]

RESULTS AND DISCUSSION

Morphology of PANI/TiO_2−SiO_2 Composites

Figure 1 displays the SEM images for (a) PANI, (b) PANI-15, (c) PANI-30, and (d) PANI-60 composites, respectively. PANI shows irregularly shaped agglomerates containing some nanofibers. Whereas, PANI/TiO_2−SiO_2 composites exhibit spherical particles. With increasing the TiO_2−SiO_2 content, the mean size of sphere-shape particles decreased. Meanwhile, the amount of the particles increased. It indicates that the TiO_2−SiO_2 hybrid fillers have a nucleus effect during the polymerization process and resulted in a homogeneous PANI shell around them. The SEM images imply that the doping of TiO_2−SiO_2 has a strong effect on the PANI's morphology. The composites show a transformation in morphology from typical fibrous PANI to particles with the increase of TiO_2−SiO_2 contents.

To obtain more detailed information of the particle morphology, PANI-60 was selected to be investigated using TEM. It can be observed that from Figure 2(a), the PANI/TiO_2−SiO_2 particles are about 200−800 nm in diameters. Floccule-like structures are also clearly visible at many places along the particle border. More detailed information about the floccule-like structures are shown in Figure 2(b) (magnified 3,00,000 times). It can be noted that the surface of the floccule-like structures is not smooth. These characteristic structures can provide large

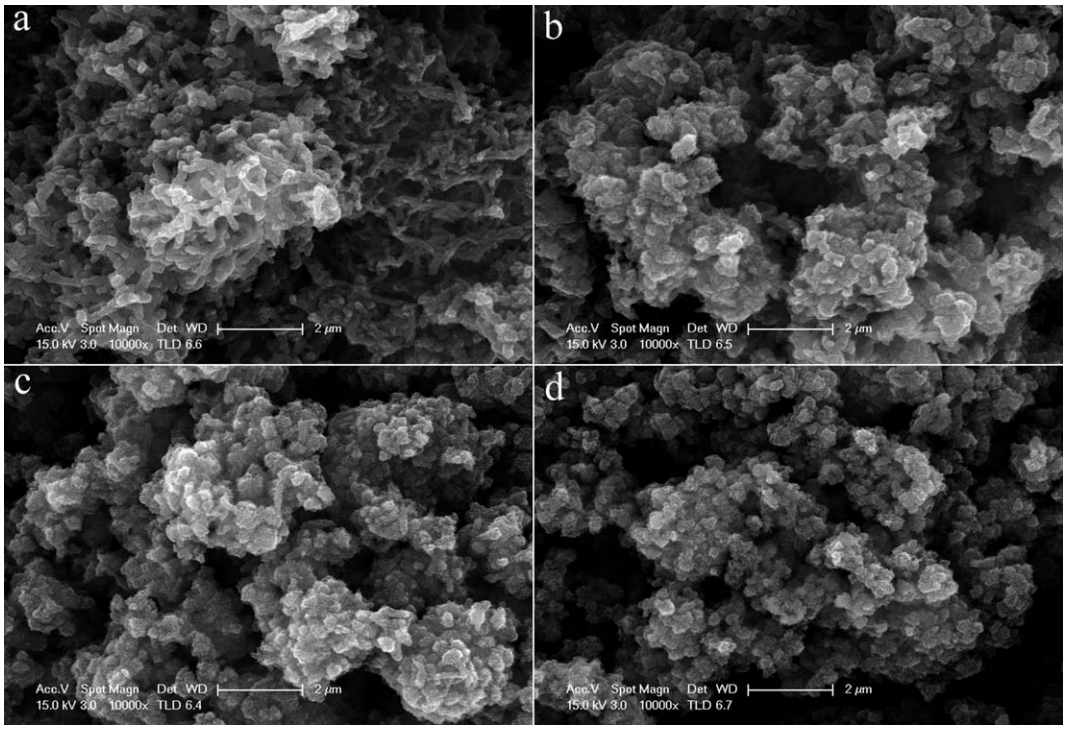

Figure 1. SEM images of the (a) PANI, (b) PANI-15, (c) PANI-30, and (d) PANI-60.

surface which may help enhance the performance of the conductive network formation for charge transport when the particles are compacted using a high pressure.

FTIR Analysis

FTIR spectra of PANI and PANI/TiO_2-SiO_2 composites are shown in Figure 3(a−e). The assignments of the main characteristic peaks of PANI are as follows. The peaks at 1572.9 and 1485.6 cm^{-1} are the characteristic of stretching modes of C=C in quinoid rings and benzenoid rings respectively. The peaks at 1291.7 and 1240.0 cm^{-1} are assigned to C−N stretching vibration of benzenoid ring. The peak at 1115.0 cm^{-1} is attributed to a plane bending vibration of C−H, which is formed during protonation.[19] The presence of absorption bands at 793.2 cm^{-1} is related to the para-substituted aromatic rings.[20] It is also noted, by comparing Figure 3(a) with Figure 3(b−e), that some peaks of PANI are shifted. For example, the peaks at 1485.6, 1291.7, and 793.2 cm^{-1} shift to higher wavenumbers slightly, while the peaks at 1572.9 and 1240.0 cm^{-1} shift to lower wavenumbers slightly. The peak at 1115.0 cm^{-1} is shifted significantly to 1107.7, 1102.0, 1099.4, and 1060.6 cm^{-1} as the increase of the percentage of TiO_2-SiO_2 particles in the composites [Figure 3(b−e)], respectively. The band at 1115.0 cm^{-1} is also lightly broadened in PANI/TiO_2-SiO_2 composites. The strong band at 1115.0 cm^{-1} was described by MacDiarmid et al. as the "electronic-like band." This is considered to be a measure of the degree of delocalization of electrons, and thus it is the characteristic peak of PANI conductivity.[21] These changes may suggest that an interaction exists between PANI macromolecule and TiO_2-SiO_2 particles.

The FTIR spectra of PANI/SiO_2 and PANI/TiO_2 are also shown in Figure 3(f) and (g), respectively. The PANI peaks at 1485.6, 1291.7, and 793.2 cm^{-1} shift to higher wavenumbers and the peaks at 1572.9 and 1240.0 cm^{-1} shift to lower wavenumbers slightly. Comparison with the neat PANI, all the characteristic peaks of PANI/SiO_2 shift to the same direction with that of PANI/TiO_2-SiO_2. The "electronic-like band" at 1115.0 cm^{-1} was noticed to be shifted to 1060.0 cm^{-1} (a lower wavenumber direction). However, in spectra of PANI/TiO_2, the band at 1115.0 cm^{-1} is shifted to a higher wavenumber direction (1126.7 cm^{-1}). During the preparation of TiO_2-SiO_2, heat treatment result in the formation of chemical Si−O−Ti bond and/or the enhancement of the adsorption of silica onto the surface of TiO_2 and thus lead to enhanced adsorption of the aniline monomer and subsequent polymerization on the TiO_2-SiO_2 surface. By comparing Figure 3(f) and (g) with Figure 3(b−e), the interaction between SiO_2 and PANI is much stronger than that between TiO_2 and PANI in the PANI/TiO_2-SiO_2 composites. The results indicate that the presence of silica on the surface of TiO_2 particles is possible.

XRD Characterization

The XRD patterns of PANI, TiO_2-SiO_2, and PANI/TiO_2-SiO_2 composites are shown in Figure 4. Curve (a) shows that the PANI has a certain degree of crystallinity. The X-ray diffraction pattern consisting of three peaks at 15°, 20°, and 25° has a similar profile as reported in the literature for polyaniline.[22–27] The peaks can be ascribed to the scattering from polyaniline chains at interplanar spacing.[26] When PANI encapsulates TiO_2-SiO_2 nanoparticles, the interaction of PANI and TiO_2-SiO_2 restricts the growth of PANI chains around TiO_2-SiO_2 nanoparticles. With increasing TiO_2-SiO_2 percentage in the composites, the crystalline behavior of PANI is hampered, and the degree of crystallinity decreases. The broad weak diffraction peaks of

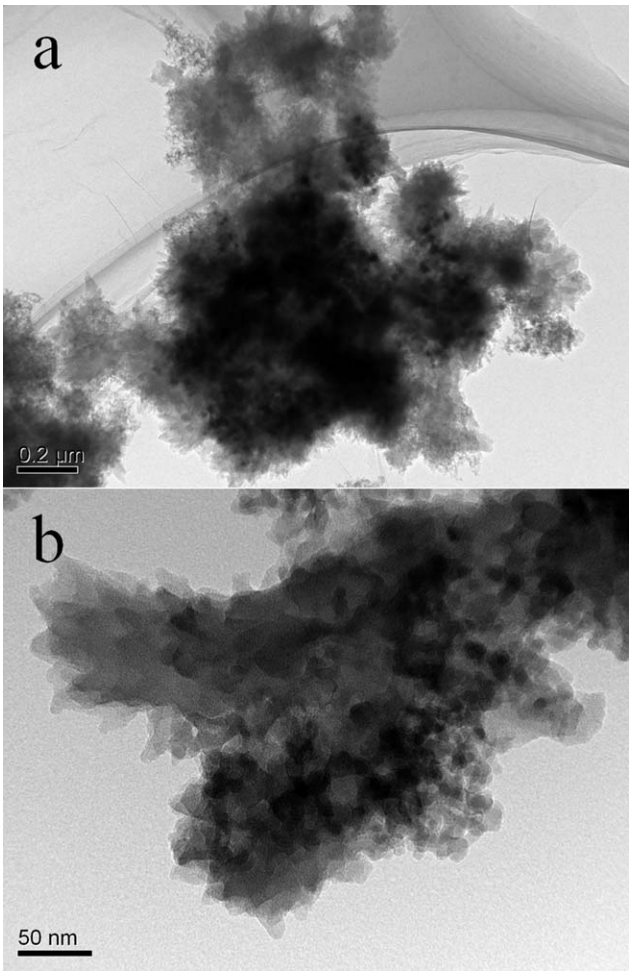

Figure 2. TEM images of the PANI-60: (a) magnified 60,000, and (b) 3,00,000 times, respectively.

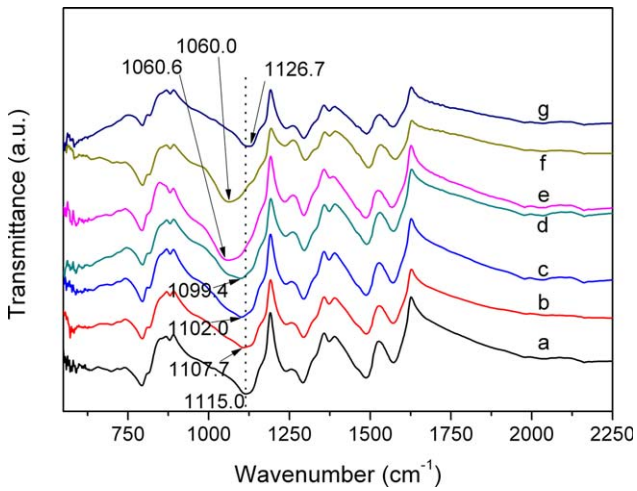

Figure 3. FTIR spectra of PANI, PANI/SiO_2, PANI/TiO_2, and PANI/TiO_2-SiO_2 composites; (a) PANI, (b) PANI-15, (c) PANI-30, (d) PANI-45, (e) PANI-60, (f) PANI/SiO_2, and (g) PANI/TiO_2. [Color figure can be viewed in the online issue, which is available at wileyonlinelibrary.com.]

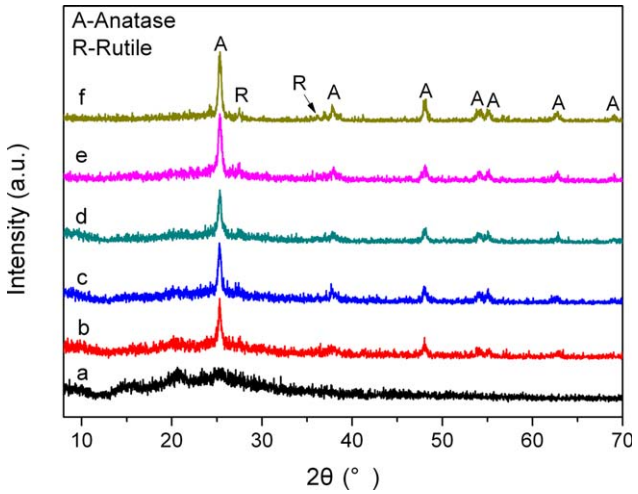

Figure 4. XRD of (a) PANI, (b) PANI-15, (c) PANI-30, (d) PANI-45, (e) PANI-60, (f) TiO_2-SiO_2. [Color figure can be viewed in the online issue, which is available at wileyonlinelibrary.com.]

PANI disappear gradually. The diffraction pattern of the TiO_2-SiO_2 composites is shown in Figure 4(f). The SiO_2 is amorphous, so that the TiO_2-SiO_2 composites only illustrate the diffraction pattern of the TiO_2.

Thermal Stability of PANI/TiO_2-SiO_2 Composites

Figure 5 shows the thermograms for PANI and PANI/TiO_2-SiO_2 composites. As can be seen, the TGA curves of these samples undergo a three-step decomposition process. It is evident that the initial mass lose below 150°C is mainly due to the release of water. The second stage loss from 240 to 350°C is possible due to the expulsion of residual dopant anions. The weight change in this stage is not evident, because all the samples were washed with large amount of water before measured ("Experimental" section). There is little residual dopant anions in all the samples, so that the pristine PANI shows similar behavior with the composites in this region. The third stage is the thermal degradation of PANI which occurs at about 400°C.

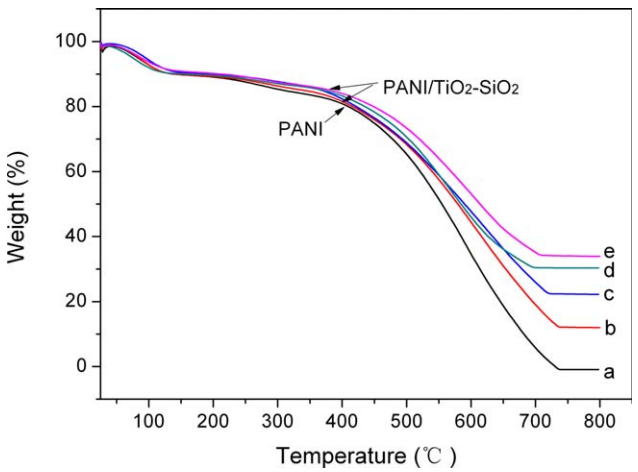

Figure 5. TGA of (a) PANI, (b) PANI-15, (c) PANI-30, (d) PANI-45, (e) PANI-60. [Color figure can be viewed in the online issue, which is available at wileyonlinelibrary.com.]

Table I. The Characteristics of PANI/TiO_2-SiO_2 Composites

Sample no.	TiO_2-SiO_2 added in the reaction mixture (g)	PANI content in the product		PANI and PANI/TiO_2-SiO_2 yield (g)
		Observed (wt %)	Expected (wt %)	
PANI	0	100	100	0.683
PANI-15	0.15	86.8	82.0	0.831
PANI-30	0.30	76.9	69.5	1.093
PANI-45	0.45	68.7	60.3	1.267
PANI-60	0.60	66.0	53.2	1.386

The temperature of thermal decomposition of PANI/TiO_2-SiO_2 composites is lower than that of PANI, which ranges from 370 to 395°C (curves b−e). The decrease of decomposition temperature can be attributed to the fact that the interaction existing at the interface between TiO_2-SiO_2 and PANI weakens the force among PANI interchains.

It can be noted that the PANI content in the PANI/TiO_2-SiO_2 composites can be obtained by evaluating the actual weight loss of the composites. The detailed characteristics of the composites with different weight percentage of TiO_2-SiO_2 are shown in Table I. The expected values of weight percentage of the PANI in the composites are estimated basing on an assumption that a constant yield of PANI (0.683 g) can be obtained under the same polymerization conditions. Compared with the actual values of weight percentage (obtain from TGA analysis), it can be suggested that the existence of TiO_2-SiO_2 increases the yield of PANI. This can be interpreted by the enhancement of the polymerization efficiency of PANI deriving from the adsorption of aniline monomer on the TiO_2-SiO_2 surface.

Charge Transport in PANI/TiO_2-SiO_2 Composites

The Current−Voltage (I−V) characteristics curves of the PANI-15 and PANI-30 between the silver and aluminum electrodes are shown in Figure 6(A) and (B). The curve is obtained by recording the readings instantaneously under a minimum pressure of 50 g/cm^2 (ensure good electrical contact between electrodes and sample). The I−V curves show non-ohmic characteristics and more detailed analysis indicate that the charge transport in PANI/TiO_2-SiO_2 is primary controlled by the Space Charge Limited Conduction (SCLC) process. In the present case, the $I-V$ relationship is in line with *eq.* (1) [28,29] as follows:

$$I=(9/8)\theta\mu\left\{V^{(n+1)}/d^{(2n+1)}\right\}. \quad (1)$$

where θ is a parameter depending on the concentration of the trapping centers, μ is the mobility of the charge carriers, V is the voltage, d is the inter-particulate distance, and n ($\geq$1) is an integer. The above relationship can be confirmed by $I-V$ curves on log−log scale which is shown in Figure 7(A) and (B). It shows that the characteristic curves are linear with two slopes (n values) viz. 1 in the low voltage region and 2−3 in the high voltage region. The voltage from which the ohmic curve transforms to non-ohmic behavior (i.e., change its slope, n value) is considered as critical voltage (V_{crit}) and is shown in Refs. 28 and 29.

$$V_{crit}=(8/9)\left\{d^{(2n)}/\theta\mu\right\} \quad (2)$$

Figure 8(A) shows the $I-V$ characteristics curves of the PANI-45 (a) with minimum mechanical pressure of 50 g/cm^2 and (b) with a mechanical pressure of 500 g/cm^2. It can be seen that the application of the mechanical pressure increases the current at a particular voltage. This can be expected since the current I in the sample has an inverse correlation to the inter-particulate distance (d), a small change in which can cause a significant change in the current value [*eq.* (1)]. It can be noted that the V_{crit} shifts to the lower voltage side [Figure 8(B)]. This may be due to that a higher conductive property reduces the charge storage at the PANI/TiO_2-SiO_2 interface. One of the most

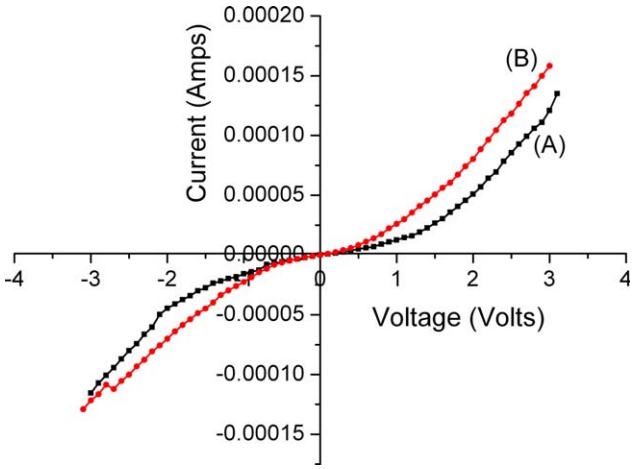

Figure 6. Current−voltage characteristics of PANI/TiO_2-SiO_2 composites: (A) PANI-15 and (B) PANI-30, with minimum pressure of 50 g/cm^2. [Color figure can be viewed in the online issue, which is available at wileyonlinelibrary.com.]

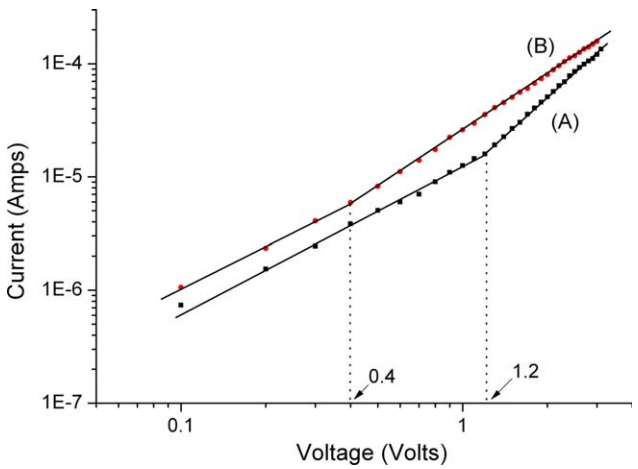

Figure 7. Log−log plot of $I-V$ characteristics of PANI/TiO_2-SiO_2 composites: (A) PANI-15 and (B) PANI-30, with minimum pressure of 50 g/cm^2. [Color figure can be viewed in the online issue, which is available at wileyonlinelibrary.com.]

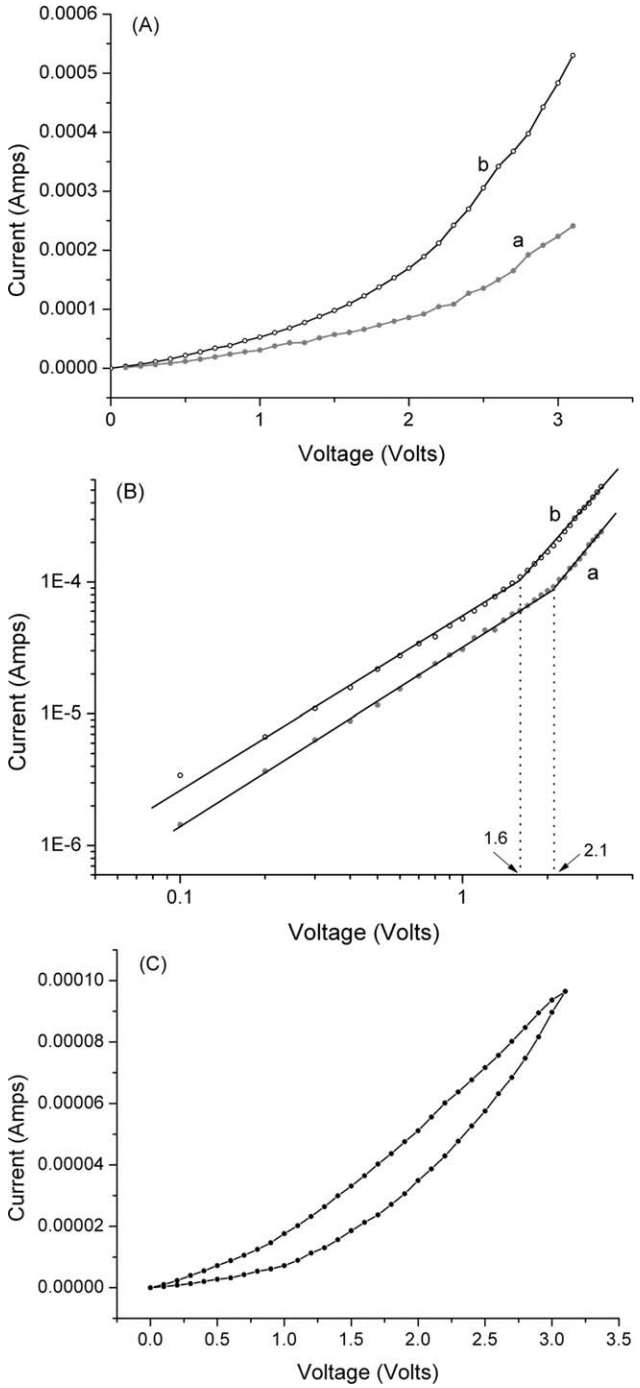

Figure 8. (A) $I-V$ characteristics curves of PANI-45: (a) with minimum mechanical pressure of 50 g/cm^2 and (b) with a mechanical pressure of 500 g/cm^2; (B) Log−log plot of $I-V$ characteristics of PANI-45: (a) with minimum mechanical pressure of 50 g/cm^2 and (b) with a mechanical pressure of 500 g/cm^2; (C) $I-V$ characteristics curves of PANI-60 with minimum mechanical pressure of 50 g/cm^2 which show a hysteresis loop.

significant characteristics of the space charge effect is the trapping and accumulation of the charge in the material. In Figure 8(C), the $I-V$ characteristic curve shows hysteresis effect, which can be attributes to charge storage in the sample. In such a case, the charge would be accumulated at the interface of PANI and TiO_2-SiO_2.

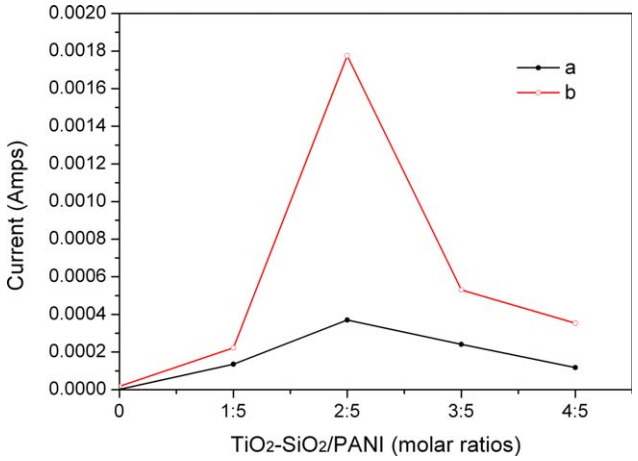

Figure 9. The current responses at 3 V of PANI/TiO_2-SiO_2 composites samples with different pressures: (a) with minimum mechanical pressure of 50 g/cm^2 and (b) with a mechanical pressure of 500 g/cm^2. [Color figure can be viewed in the online issue, which is available at wileyonlinelibrary.com.]

Electrical Conductivities of PANI/TiO_2-SiO_2 Composites

The electrical conductivities of these PANI/TiO_2-SiO_2 composites show pressure sensitivity properties. The current responses at 3 V of PANI/TiO_2-SiO_2 composites samples with the minimum mechanical pressure of 50 g/cm^2 and a mechanical pressure of 500 g/cm^2 pressure are shown in Figure 9. It is clearly seen that the pressure sensitivity is maximum when the initial TiO_2-SiO_2/ANI molar ratio is 2 : 5. Approximate electrical conductivity was obtained by analyzing the $I-V$ characteristics curves. As can be seen, the conductivity of PANI/TiO_2-SiO_2 composites greatly increases with an increase in TiO_2-SiO_2 content (from initial TiO_2-SiO_2/ANI molar ratio of 1 : 5 to 2 : 5) and reaches a maximum value at the ratio of 2 : 5. This enhanced conductivity is perhaps due to the dopant effect of TiO_2-SiO_2 and/or the interaction existing between PANI and TiO_2-SiO_2 particles. Beyond this point, with amount of

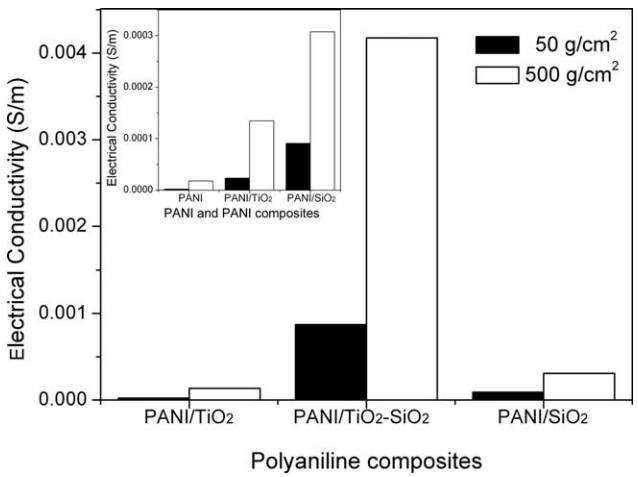

Figure 10. The electrical conductivity of PANI/TiO_2-SiO_2, PANI/TiO_2, and PANI/SiO_2; neat PANI, PANI/TiO_2, and PANI/SiO_2 (the inset) with minimum mechanical pressure of 50 g/cm^2 and with a mechanical pressure of 500 g/cm^2.

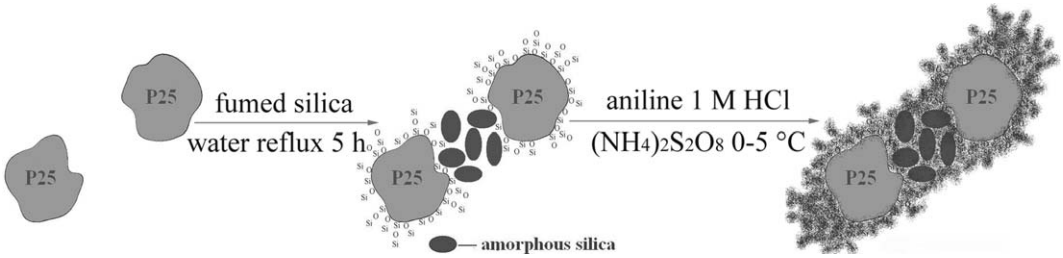

Figure 11. Simple scheme of PANI/TiO_2-SiO_2 composites preparation.

percentage TiO_2-SiO_2 content increasing, the conductivity gradually declines. The decrease in conductivity may be due to particle blockage of conduction path by the nanoparticles embedded in the PANI matrix.

To investigate the conductive characteristics of the PANI/TiO_2-SiO_2 composites, PANI/TiO_2 (with a middle initial TiO_2/ANI molar ratio of 1 : 2), PANI/SiO_2 (the initial SiO_2/ANI molar ratio is 1 : 2), and neat PANI were synthesized under the same condition. Figure 10 and its inset show the electrical conductivity of the PANI composites and neat PANI. The histograms clearly illustrate that the electrical conductivity of PANI composites are all much higher than that of the neat PANI and the conductivity of PANI/TiO_2-SiO_2 (with initial TiO_2-SiO_2/ANI molar ratio of 2 : 5) is at least one order of magnitude greater than that of PANI/TiO_2 and PANI/SiO_2, respectively, no matter the addition pressure is applied or not. In our experiment, the weight percentage of TiO_2 (or SiO_2) in PANI/TiO_2 (or PANI/SiO_2) is 30.33% (or 24.67%). Though these values may not be the optimal ratios for conductivity, PANI/TiO_2 (or PANI/SiO_2) also exhibits relatively high conductivity properties (several times higher than that of pristine PANI). Moreover, we found that the conductivities of PANI/TiO_2 (or PANI/SiO_2) composites always vary in an order of magnitude[1,2,13,16] and the lowest conductivity value of PANI/TiO_2-SiO_2 composites (PANI-60, 2.840E−4 S/m without additional pressure; PANI-15, 5.452E−4 S/m with additional pressure of 500 g/cm^2) is higher than that of PANI/TiO_2 and PANI/SiO_2, respectively. This significant enhancement in conductivity of PANI/TiO_2-SiO_2 is due to the instinct properties of the TiO_2-SiO_2 composite rather than its percentage in the composites.

An doping effect associated with TiO_2 nanoparticles was believed to help induce the conductive network formation and, thus, enhance the electrical conduction of PANI/TiO_2.[30] During the preparation of TiO_2-SiO_2, some chemical Si−O−Ti bond may be generated and/or adsorption of fumed silica onto the surface of TiO_2 may be enhanced by the heat treatment. When the TiO_2-SiO_2 composite was used as starting sites for polymerization of aniline, the fumed silica existing on the surface of TiO_2/connecting the TiO_2 particles can adsorb aniline molecules and generate "conducting bridges" connecting PANI conducting domains and increasing the effective penetration which can be confirmed by the FTIR results.[2] Because of the exist of the TiO_2 backbone, the conductive network of PANI/TiO_2-SiO_2 is more orderly and effective. Also, the floccule-like structures provide large surface which may help enhance the performance of the efficient network and may promote the extent of conjugation of PANI conducting domains for charge transport. On the basis of the discussion, a schema of PANI/TiO_2-SiO_2 structure can be proposed and is shown in Figure 11. The high conductivity of PANI/TiO_2-SiO_2 is also related to the synergy effect between TiO_2 and fumed silica in the polymerization process. These conducting PANI/TiO_2-SiO_2 composites whose charge transport is mainly controlled by space charge may be promising candidates for advanced materials to be used in the high-technology industries in the future. And more detailed information about their electrical conductive mechanism needs further studies.

CONCLUSIONS

Conducting polyaniline PANI/TiO_2-SiO_2 composites have been synthesized by an *in situ* method. The presence of hybrid TiO_2-SiO_2 in the composites results in a variation in microstructure, which implies a strong interaction between the fillers and PANI matrix. The interaction was also evidenced through FTIR spectroscopy analysis. The $I-V$ characteristics in such composites reveal that the charge transport process is mainly governed by the space charge effects (occur at the interface between the conducting PANI and TiO_2-SiO_2). Large hysteresis observed in the $I-V$ characteristics also supports the SCLC type charge transport mechanism. These PANI/TiO_2-SiO_2 composites show dramatically enhanced conductivity as compared to the pristine PANI, PANI/TiO_2, and PANI/SiO_2. The enhanced conductivity may be due to the synergy effect of TiO_2-SiO_2 and/or the interaction existing between PANI and TiO_2-SiO_2 particles.

ACKNOWLEDGMENTS

The authors gratefully acknowledge the support of the National Natural Science Foundation of China (Nos. 21174108, 11205118) and "the Fundamental Research Funds for the Central Universities" (No.20102020201000017).

REFERENCES

1. Su, S. J.; Kuramoto, N. *Synth. Methods* **2000**, *114*, 147.
2. Zengin, H.; Erkan, B. *Polym. Adv. Technol.* **2010**, *21*, 216.
3. Lira-Gantu, M.; Gomez-Romero, P. *J. Solid State Chem.* **1999**, *147*, 601.
4. Somani, P. R.; Marimuthu, R.; Mulik, U. P.; Sainkar, S. R.; Amalnerkar, D. P. *Synth. Methods* **1999**, *106*, 45.
5. Somani, P. R.; Kale, B. B.; Amalnerkar, D. P. *Synth. Methods* **1999**, *106*, 53.

6. Epstein, A. J.; MacDiarmid, A. G. *Makromol. Chem. Macromol. Symp.* **1991**, *51*, 217.
7. Heinze, J. *Top. Curr. Chem.* **1990**, *152*, 2.
8. Yang, Y.; Heeger, A. *J. Appl. Phys. Lett.* **1994**, *64*, 1245.
9. Unde, S.; Ganu, J.; Radhakrishnan, S. *Adv. Mater. Opt. Electron.* **1996**, *6*, 151.
10. Somani, P. R.; Radhakrishnan, S. *Chem. Phys. Lett.* **1998**, *292*, 218.
11. Somani, P. R.; Mandale, A. B.; Radhakrishnan, S. *Acta Mater.* **2000**, *48*, 2859.
12. Somani, P. R.; Marimuthu, R.; Mandale, A. B. *Polymer* **2001**, *42*, 2991.
13. Xu, J. C.; Liu, W. M.; Li, H. L. *Mater. Sci. Eng. C* **2005**, *25*, 444.
14. Basavaraja, C.; Kim, N. R.; Jo, E. A.; Huh, D. S. *Polym. Compos.* **2010**, *31*, 1754.
15. Xia, H.; Wang, Q. *J. Appl. Polym. Sci.* **2003**, 87, 1811.
16. Li, X.; Dai, N.; Wang, G.; Song, X. *J. Appl. Polym. Sci.* **2008**, *107*, 403.
17. Radhakrishnan, S.; Saini, D. R. *Synth. Methods* **1993**, *58*, 243.
18. Radhakrishnan, S.; Khedkar, S. P. *Synth. Methods* **1996**, *79*, 219.
19. Kang, E. T.; Neoh, K. G.; Tan, K. L. *Prog. Polym. Sci.* **1998**, *23*, 277.
20. Basavaraja, C.; Veeranagouda, Y.; Lee, K.; Pierson, R.; Huh, D. S. *J. Polym. Sci. Part B: Polym. Phys.* **2009**, *47*, 36.
21. Quillard, S.; Louarn, G.; Lefrant, S.; MacDiarmid, A. G. *Phys. Rev. B* **1994**, *50*, 12496.
22. Abdiryim, T.; Gang, Z. X.; Jamal, R. *Mater. Chem. Phys.* **2005**, *90*, 367.
23. Wan, M.; Li, J. *J. Polym. Sci. Part A: Polym. Chem.* **1998**, *36*, 2799.
24. Lee, K.; Cho, S.; Park, S. H.; Heeger, A. J.; Lee, C. -W.; Lee, S. -H. *Nature* **2006**, *441*, 65.
25. Yang, X.; Li, B.; Wang, H.; Hou, B. *Prog. Org. Coat.* **2010**, *69*, 267.
26. Feng, W.; Sun, E.; Fujii, A.; Wu, H.; Nihara, K.; Yoshino, K. *Bull. Chem. Soc. Jpn.* **2000**, *73*, 2627.
27. Li, X.; Li, X.; Wang, G. *Appl. Surf. Sci.* **2005**, *249*, 266.
28. Gutman, F.; Lyons, L. E. Organic Semiconductors; Wiley: New York, **1982**.
29. Scnor, D. A. Electrical Properties of Polymers; Academic Press: New York, **1982**.
30. Armes, S. P.; Gottesfeld, S.; Beery, J. G.; Garzon, F.; Agnew, S. F. *Polymer* **1991**, *32*, 2325.